Residual Stress Control Issues for Thermal Deposition of Polymers in SFF Processes

Raymond Ong and Jack Beuth
Department of Mechanical Engineering
Carnegie Mellon University
Pittsburgh, PA

Lee Weiss
Robotics Institute
Carnegie Mellon University
Pittsburgh, PA

Abstract

Controlling residual stress-induced warping and other tolerance losses is important for accurately creating parts by solid freeform fabrication (SFF). In this paper, results are presented from warping experiments on plate-shaped acrylonitrile butadiene styrene (ABS) specimens created by an extrusion process used in Shape Deposition Manufacturing (SDM). Experimental results are compared to predictions from both one- and two-dimensional types of residual stress models. In addition to SDM, methods and results from this study are applicable to a number of other solid freeform fabrication processes involving extrusion of polymers or polymer slurries. Results from polymer extrusion are compared with those from existing work on thermal deposition of metals. Unlike metals, polymer deposition shows essentially no stress reduction due to preheating by the deposition process. Due to a greater number of deposited rows, directionality of warping is also greater than in metals. Polymer deposition experiments show that a preheat temperature near the glass transition temperature is needed for essentially no warping. Comparison of predicted and measured curvatures show that a simple 1-D thermomechanical model does not predict warping magnitudes well, but does provide insight into trends in warping as a function of preheat temperature. The effects of successive material deposition are substantial in this process and a 2-D model that includes the effects of successively deposited rows can provide much more accurate curvature predictions.

Introduction

Solid freeform fabrication (SFF) processes allow the automated building of parts of complex geometry directly from 3-D computer-aided design (CAD) models without part-specific tooling or human intervention. Many SFF processes are currently in commercial use, while others are being refined at universities and national laboratories. There are several commercially available SFF systems, including Stereolithography (3-D Systems, http://www.3dsystems.com), PatternMaster and ModelMaker inkjet systems (Sanders Prototype, http://sanders-prototype.com), Fused Deposition Modeling (Stratasys, Inc., http://www.stratasys.com) and Selective Laser Sintering (DTM Corporation, http://www.dtm-corp.com).

Shape Deposition Manufacturing (SDM) is an SFF process currently under development at Carnegie Mellon University (Merz et al., 1994) and Stanford University (Fessler et al., 1996). The SDM process combines layer deposition with incremental computer numerically controlled (CNC) machining for accuracy. SDM utilizes a variety of materials including ceramics, waxes, polymers and metals. Several methods have been investigated for the deposition of these

materials; these include microcasting, conventional welding and laser deposition for metals, extrusion for thermoplastics and casting for two-part resin systems and waxes. This paper considers polymer extrusion. In this study, the polymer material used is acrylonitrile butadiene styrene (ABS). Because it exhibits good bonding characteristics, good dimensional stability and is chemically resistant, it is one of the most common polymer materials used in SFF systems. Extrusion techniques can also be applied to the deposition of other materials, such as polymer/ceramic slurries for the creation of green ceramic parts.

One of the main issues that limits the quality of parts made by this and other extrusion processes is residual stress-induced warping. This includes processes involving slurry deposition, where stress- and distortion-free green parts are needed. When stresses are not well controlled, they can act to limit finished part size because total deflections (loss of tolerances) generally scale with part size. Currently, uniform substrate heating is the most common approach used to reduce warping in commercial SFF processes. Previous work on deposition of stainless steel (Klingbeil, 1998; Klingbeil et al., 1998, 2000) shows a number of subtleties in controlling stress-induced part warping. In metal deposition, substrate preheating and substrate insulation can give substantial payoffs in limiting residual stresses. In this paper, methods are presented for measuring and modeling warping of polymer parts, with the goals of understanding warping control via preheating for polymers and comparing it to stress control for metals.

Warping Experiments

Extrusion System: The polymer extrusion system used within SDM deposits parts via a high-pressure plunger-type extruder supplied by the Advanced Ceramic Research Corporation. The extruder contains a stainless steel barrel, which functions as a reservoir for a polymer feed rod. An actuator-controlled piston in the barrel is used to push material downward. A nozzle adapter clamped to the bottom edge of the barrel is covered with a heating element and functions as a heating zone to melt the feed rod material. For ABS the flowable material is extruded through a 0.508 mm diameter nozzle tip at a deposition rate of approximately 6.35 mm/s. After each layer is extruded, it is precisely machined to shape in a CNC milling machine.

Warping Experiments: In this study, an experimental technique is used for measuring warping in plate-shaped deposits that has been adapted from previous tests involving deposition of 304 stainless steel (Klingbeil, 1998; Klingbeil et al., 1997, 1998, 2000). The test configuration used for extruded ABS is shown in Fig. 1. For all the specimens, the 152 x 152 x 3.18 mm substrate was cut from standard 305 x 305 x 3.18 mm ABS sheet. Warping of specimens during the deposition process is not allowed. The ABS substrate was constrained from warping by an aluminum frame, with each of the eight equally spaced screws used to attach the frame to a 19 mm thick mounting plate tightened to 1.13 N·m. The deposition path was as shown in Fig. 1, where the extruder began at the negative x, positive y corner and continued in a raster pattern parallel to the x direction until ending in the negative x, negative y corner. Approximately 100 rows were extruded to create a 102 x 102 mm deposit.

Following material deposition, the specimen was allowed to cool to room temperature, and the deposit was machined flat to a thickness of 0.80 mm. Measurements were taken at 81 equally spaced points forming a 102 x 102 mm grid on the surface of the deposit. Upon completion, the specimen was unscrewed from both the aluminum frame and mounting plate, leaving one corner constrained. Warping deflection measurements were taken at the same 81

equally spaced points. All measurements were made using a dial gauge with the CNC milling machine, with an accuracy of ±2.54 μm.

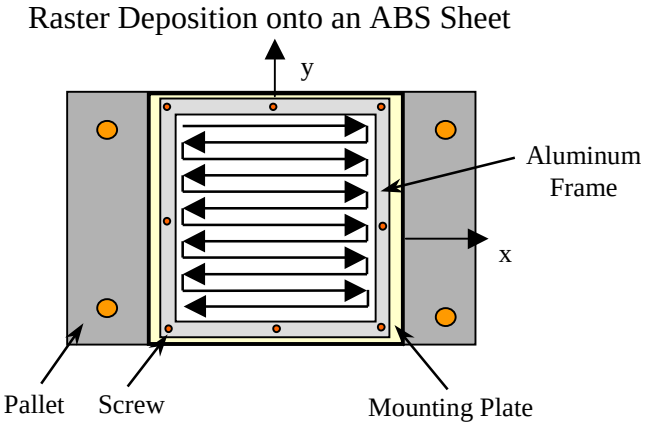

Figure 1. Warping Test Specimen Configuration for ABS Specimens

Typical Experimental Results: After obtaining measurements of warping deflections, the curvatures in the x and y directions were calculated using 2-D polynomial least square fits of the displacement data following the work of Klingbeil (1998) and Klingbeil et al. (1998, 2000). A 2-D polynomial surface w(x,y) was determined by a least square fit of the measured data as shown in Fig. 2, after which the curvatures $\frac{\partial^2 w}{\partial x^2}$ and $\frac{\partial^2 w}{\partial y^2}$ were obtained by analytical differentiation of the function w(x,y). Second order fits result in constant curvatures, which can be interpreted as average curvatures in the x and y directions. Third order fits allow a bilinear variation in curvatures in the x and y directions, which can be used to illustrate deposition path effects. All curvature results are normalized by κ_{max} = 0.222 in^{-1}, the maximum theoretical curvature corresponding to release of a fully plastic biaxial moment with an assumed room-temperature yield stress of 26.5 MPa.

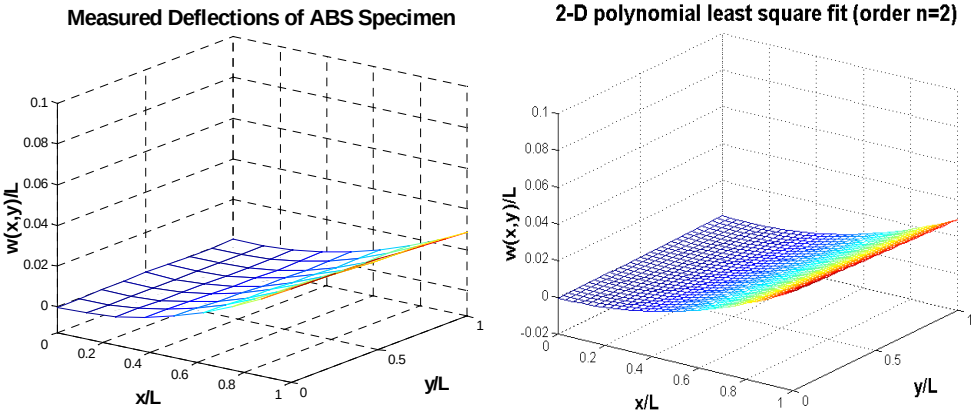

Figure 2. Measured Results and Fitted Displacement Results for the Substrate at 27°C

Average (second order) curvature results show that warping magnitudes parallel to the deposition direction are significantly larger than warping magnitudes transverse to the deposition direction, which are near zero (this can also be seen qualitatively in the plots of deflections in Fig. 2). This is due to the effects of free surfaces in new material as it is deposited in rows and

thermal cycling of the substrate, which is periodic in the y direction. Both of these effects act to reduce average stresses in the transverse direction that lead to transverse curvatures. This effect is also seen in metal deposition processes and its magnitude is dependent on the number of deposited rows used per unit length in the y direction. For stainless steel deposition by the microcasting process in SDM, 102 mm can be filled with roughly 20 rows, compared to the 100 rows needed for extruded ABS. As a result, the differences in warping in the x and y directions clearly exist, but are much more subtle in the deposition of stainless steel.

Third order results show that there is essentially no change in warping magnitudes in the x or y direction as polymer deposition progresses across the substrate (see Fig. 3). This is unlike what is seen in metal deposition, where warping curvatures decrease significantly as deposition progresses, due to substrate preheating by previously deposited material. In polymer extrusion, there is no significant heating of the substrate by previously deposited material; substrate temperatures before deposition begins and after it is completed differ by $\approx 2^{o}C$ at most. Therefore, to control residual stress in polymer parts by part preheating, heat must be supplied to the substrate throughout the deposition process. In comparison, for metal deposition, an initial preheating and part insulation can achieve stress control, so that the process itself contributes much of the thermal energy for substrate preheating.

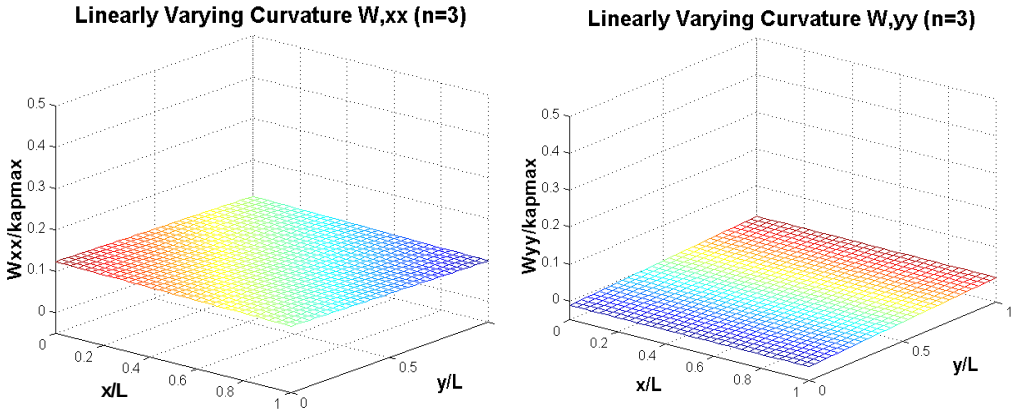

Figure 3. Linearly Varying Curvature Results for the Substrate at $27^{o}C$

Numerical Models

During ABS deposition, the deposit and substrate are constrained from warping and the resulting residual stress state is determined by high-temperature, non-linear material response. Following manufacture, the plate is released from its constraints, which results in primarily elastic unloading. With reference to previous work by Chin et al. (1996), Klingbeil (1998) and Klingbeil et al. (1998, 2000), two types of finite element thermomechanical models are used to model the constrained stress state for a thin layer of ABS deposited onto an ABS substrate. The commercial software package ABAQUS is used for the thermal and mechanical simulations for both model types. Because the release of constraint results in primarily elastic unloading, the corresponding warping deformation may be calculated by an elastic analysis.

1-D Model: A schematic of the 1-D thermomechanical model and boundary conditions used in this study is shown in Fig. 4 (see Chin et al., 1996). The result of its thermal and mechanical assumptions is that layer deposition is modeled as if all of the extruded material is deposited at once, neglecting the effects of incremental deposition of individual rows. The

thermal model is one-dimensional, consisting of a column of 1-D quadratic thermal elements. The thermal boundary condition on the top surface is convection. The thermal boundary conditions on the bottom surface of the substrate are prescribed with a constant temperature equal to the preheat temperature. In the thermal model, the assumption is made that the deposit thoroughly wets the substrate, so no contact resistance against heat flow is specified at the initial deposit and substrate interface.

The 1-D mechanical model is axisymmetric, with boundary conditions specified such that temperatures from the 1-D thermal model result in equal biaxial residual stresses that are a function of time and the axial (z) coordinate only. The mechanical boundary conditions are such that the deposit and substrate are constrained from bending, but support no net force. Radial displacements along r = 0 (the model centerline) are set equal to zero. The external vertical substrate and deposit surfaces are required to remain vertical, and they are permitted to uniformly displace in a horizontal direction. The top surface of the deposit is traction free, and a zero axial displacement ($u_z = 0$) is prescribed on the bottom surface of the substrate. A perfect bond between the deposit and the substrate is assumed. The mesh resolution used in the thermal and mechanical models has been verified by doubling their resolution, which produced intangible changes in plotted temperatures and stresses. The final constrained stress distribution as a function of z includes a net bending moment. Release of this bending moment results in elastic unloading and warping. The bending moment is related to the warping curvatures $\frac{\partial^2 w}{\partial x^2} = \frac{\partial^2 w}{\partial y^2} = \kappa$ through elastic plate theory. Homogenous plate equations are suitable since the deposit and the substrate are ABS.

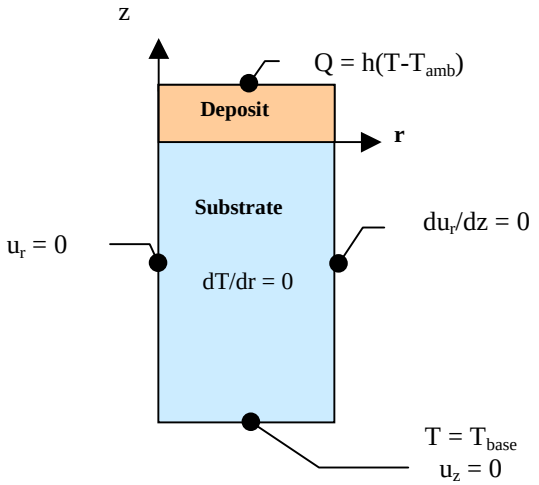

Figure 4. Boundary Conditions on the 1-D Thermomechanical Model

2-D Successive Row Model: 2-D thermal and 2-D generalized plane strain (GPS) models are used to simulate some of the deposition path effects present during actual material deposition (see Klingbeil (1998) and Klingbeil et al. (1998, 2000)). These models account for the effects of deposited rows; however, they still model single rows as being deposited at once. A time delay between deposition of each row is used to approximate the real-time experiments. During a simulation, each successively deposited row is "bonded" to the adjacent row and the substrate by matching the temperatures and displacements of corresponding nodes. A typical finite element mesh and the model boundary conditions are depicted in Fig. 5. The coordinates are chosen to be consistent with those used for the experiments, where the x-direction is perpendicular to the page.

A GPS model assumes that the 2-D model lies between two rigid bounding planes, which are normal to the x direction. These two planes can move with respect to each other and hence cause a uniform axial displacement u_x, as well as relative rotations per unit length ϕ_y and ϕ_z about the y and z axis, respectively. Rigid body movement of the two planes results in an axial strain ε_{xx} that varies linearly in y and z.

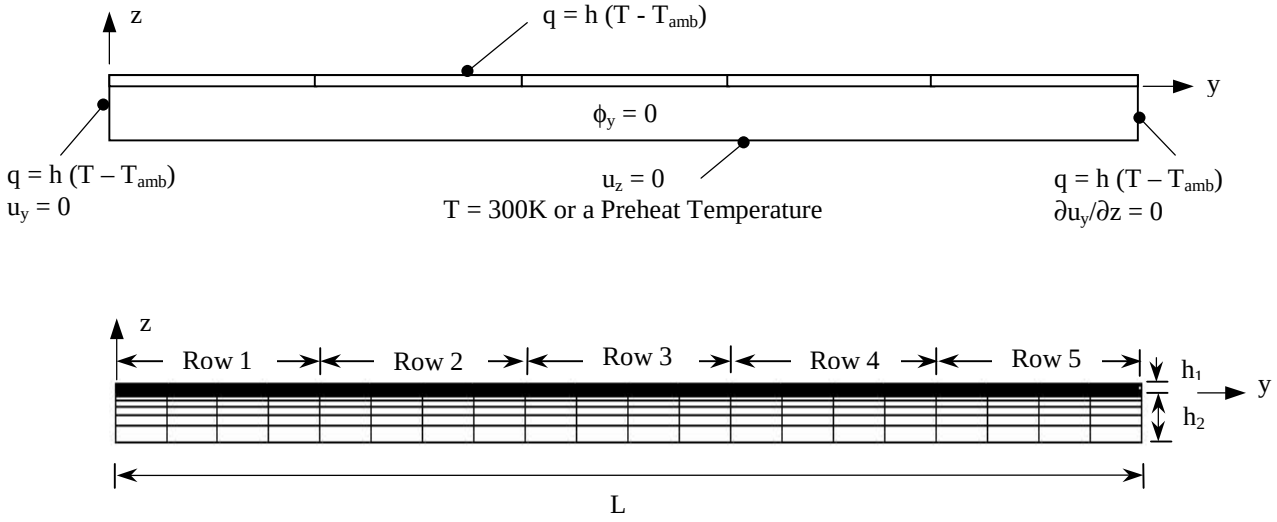

Figure 5. Boundary Conditions and Finite Element Mesh of a Generalized Plane Strain Model

As shown in Fig. 5, the boundary conditions used for the GPS model are analogous to the constrained conditions used in the 1-D modeling. Both the left and right edges of the model are constrained to be vertical, while the bottom surface is constrained to have no displacement in the z-direction. During material deposition, the rigid rotation ϕ_y is constrained. These mechanical constraints are chosen to approximate the conditions of the experiments. After material deposition and cooling to room temperature, the warping deformation is obtained in a separate solution step by releasing both the in-plane and the out-of-plane constraints. The uniform curvature $\frac{\partial^2 w}{\partial x^2}$ in the x-direction is given by the subsequent rotation per unit length ϕ_y. The numerical plate deflections $w_o(y) = w(x = 0, y)$ are extracted from the deflections along the top of the modeled deposit, over the region $0 \le x \le L$. The displacements as a function of x and y are thus determined to within a rigid body displacement as

$$w(x, y) = \frac{\varphi_y}{2} x^2 + w_o(y) . \qquad (1)$$

Numerical results for average and linearly varying curvatures in the x and y directions are then obtained from 2-D polynomial least square fits of w(x,y).

In the thermal modeling, the properties that are set to depend on temperature are density (Brandrup and Immergut, 1989), specific heat (Bair, 1970) and conductivity (Brandrup and Immergut, 1989). Room temperature values for density and conductivity were also provided by the ABS supplier, McMaster-Carr. Ideally, material properties used in the mechanical analyses would include viscoelastic and creep effects; however, existing data in the literature is limited, even for a widely used thermoplastic like ABS. Thus, in the mechanical analyses, both the deposit and substrate are assumed to have elastic-perfectly plastic constitutive behavior. The mechanical properties that are set to depend on temperature are elastic modulus (Locati et al.,

1996) and yield stress, with the rate dependence of yield stress included (Imasawa and Matsuo, 1970). Room temperature values of elastic modulus and yield stress were also provided by McMaster-Carr. The elastic Poisson's ratio is set to be equal to 0.35, independent of temperature. The linear thermal expansion coefficient is specified as 9.5 x 10^{-5} ε/K (Murray, 1997). The melting temperature is roughly 115°C and the glass transition temperature, T_g, is roughly 94°C (Bair, 1970).

Measured and Predicted Warping vs. Preheat Temperature

Experimentally determined curvatures are plotted vs. preheat temperature in Fig. 6, where plotted values are the average of the curvatures in the x and y directions, and the curvature in each direction is averaged over the plate from use of a second order fit to the displacement data. The experiments show an essentially linear dependence of final curvature magnitudes on preheat temperature. This allows straightforward extrapolation of the measured results to obtain a preheat temperature for zero curvature equal to 84°C. This is close to the glass transition temperature of the ABS polymer (≈ 94°C), and is also close to the melting point (≈ 115°C). In contrast, for deposition of stainless steel, the preheat temperature for zero curvature is on the order of two thirds of the absolute melting temperature.

Predicted curvatures for various preheat temperatures are also plotted in Fig. 6, as determined using the 1-D model. As previously noted, in the 1-D model it is assumed that the warping is equal in both the x and y directions. Results for two different yield stress vs. temperature behaviors are presented. Available yield stress vs. temperature data for ABS is in the range -40 to 60°C. Properties at higher temperatures must be extrapolated from this measured data. The line at the top of the plot resulted from a first attempt at extrapolation of this data, which resulted in a temperature for $\sigma_Y = 0$ of 92°C. However, this resulted in a prediction of preheat temperature for no warping curvature (also equal to 92°C) that did not match the experiments. The second predicted line was obtained with an extrapolation that yielded a temperature for $\sigma_Y = 0$ of 84°C, consistent with the experimental warping vs. temperature data. Because this extrapolation was also consistent with the yield stress data in the range of -40 to 60°C, this was chosen as the final yield stress vs. temperature behavior to be used in the modeling of this study. This rather modest change in the material properties input to the model resulted in a noticeable change in the predicted warping magnitudes. Thus the modeled properties near the glass transition temperature can have a significant effect on predicted warping magnitudes.

One key issue is that both the experiments and 1-D model show an essentially linear decrease in curvature with temperature. In the predictions, this can be explained as being due to the yield stress vs. temperature behavior used in the numerical model. As the deposit cools to temperatures just below T_g, the yield stress in this material becomes greater than the maximum stress due to thermal mismatch, and it stays that way as the deposit cools. Hence, much of the stress build-up in the deposit and substrate is nearly linear (proportional to $E\alpha\Delta T$ but with a temperature-dependent Young's modulus). Thus stress build-up in this polymer system is largely linear elastic, but magnitudes are a function of the nonlinear properties near the glass transition temperature.

Although the 1-D model appears to be capturing some of the physics of the experiments (the linear variation of warping with preheat temperature), it is clearly doing a poor job of predicting warping magnitudes. This is even true with the somewhat fitted yield stress vs. temperature behavior for T > 60°C. This could be due to the material model not including

viscoelastic stress relaxation that may be occurring in the experiments. It could also be due to the simplistic geometry of the 1-D model, which does not simulate the successive deposition of extruded material.

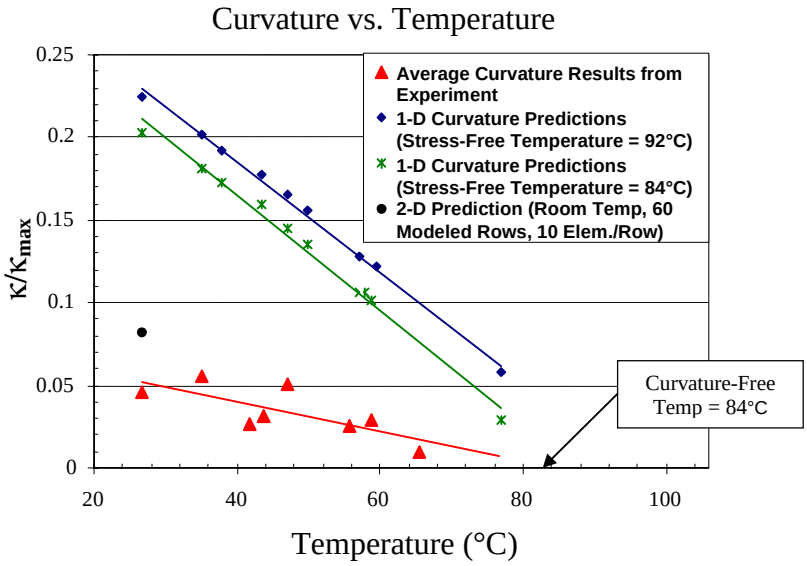

Figure 6. Plot of Measured and Predicted Curvature versus Preheat Temperature

The 2-D successive row model has been used to simulate the effects of successive material deposition. In the actual deposition process it takes approximately 100 rows to deposit a 102 x 102 mm surface. A fully refined model of deposition of this many individual rows is possible, but computationally impractical. Therefore, numerical simulations with various numbers of deposited rows and levels of mesh resolution have been carried out for deposition onto a room temperature substrate. A plot of the results as a function of the number of deposited rows is shown in Fig. 7, where a result with a single deposited row matches the prediction of the 1-D model to within 5%. The experimentally measured warping curvature for a room temperature substrate is shown as a dashed line at the bottom of the plot.

Most of the data in Fig. 7 is for a model with 10 elements (5 in the z direction and 2 in the y direction) discretizing each row. From this series of simulations (with 10 elements per row) it is clear that the predicted warping magnitudes decrease significantly as the number of modeled rows of deposit increases. The curvature prediction for successive deposition of 60 rows is less than half that of the 1-D model (this result is also plotted in Fig. 6). Although results from a simulation of 100 rows are not included in Fig. 7, it is clear that much of the discrepancy between the 1-D predictions and the experiments (which show some scatter) can be explained by the need to model successive material deposition. Two results are also plotted in Fig. 7 for deposited rows discretized by 5 elements in the z direction and 4 elements in the y direction. It appears that there is some effect of mesh resolution on the results, but it is not large, and is not a strong function of the number of modeled rows. In addition, the differences in curvature values in the x and y directions obtained from the successive row model agree with those seen in the experiments. Both show that warping is greater in the direction of deposition. Hence, the 2-D successive row model appears able to provide much more reasonable predictions of warping magnitudes and is able to capture deposition path effects evident in the experiments.

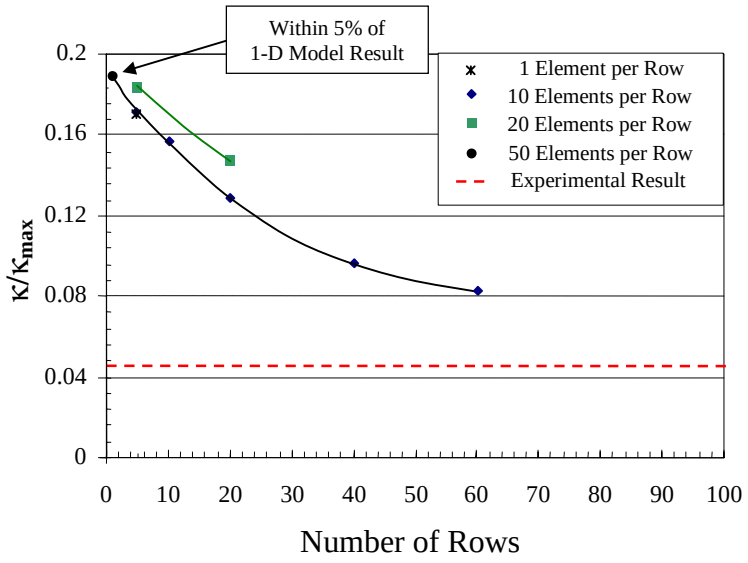

Figure 7. Warping Magnitudes vs. Number of Modeled Rows for a 300K Substrate

Conclusions

The control of residual stress-induced warping has been considered for polymer deposition-based SFF processes, through the study of a polymer extrusion process using ABS. Warping experiments have demonstrated a number of physical differences between these processes and analogous processes involving metal deposition. First, significantly more directionality of warping is seen for polymer deposition than metal deposition. In fact, the experiments show essentially no curvature in the direction transverse to the deposition direction. This is likely due to the significantly greater number of rows used in the polymer deposition process studied, which increases free-edge and other effects in the transverse direction. There is also no change in warping magnitudes as polymer deposition progresses across the substrate. This is unlike what is seen in metal deposition, where warping curvatures decrease as deposition progresses, due to substrate preheating by previously deposited material. To control residual stresses in polymer deposition processes by preheating, heat must be supplied to the substrate throughout the deposition process. In contrast, for metal deposition, an initial preheating and part insulation can achieve stress control. Warping measurements show an essentially linear dependence of final curvature magnitudes on preheat temperature, which allows straightforward extrapolation to a preheat temperature for no warping. This temperature is near the glass transition temperature and is also close to the melting point. In comparison, for metal deposition processes, the preheat temperature for zero curvature is on the order of two thirds of the absolute melting temperature.

Results from the modeling portion of this study provide insight into why an essentially linear relationship exists between warping magnitudes and preheat temperature. The final residual stress magnitudes needed to cause substantial warping in ABS are significantly smaller than the yield stress at room temperature. In fact, when the maximum temperature in the deposit and substrate is just below the glass transition temperature, the yield stress becomes greater than the maximum stress due to thermal mismatches. From this point on, stress build-up in the deposit and substrate is nearly linear (with a temperature-dependent Young's modulus). This results in stress magnitudes that are essentially proportional to changes in preheat temperature. Both 1-D and 2-D successive row deposition models have been successful in predicting trends in the

experimental observations and in giving insight into the experiments. However, 2-D model warping predictions presented herein are much closer to measured values, and simulations including the 100 rows deposited in the experiments should be even closer. This is due to the 2-D model accounting for successive row deposition effects, which are significant for this process.

Acknowledgements

The authors gratefully acknowledge financial support from the Gintic Institute of Manufacturing Technology and from the National Science Foundation, under grant DMI-9700320. A software grant from SDRC allowed use of their software for finite element pre- and post- processing.

References

1. Bair, H.E. (1970) "Quantitative Thermal Analysis of Polyblends," *Polymer Engineering and Science*, Vol. 10, No. 4, pp. 247-250.
2. Brandrup, J. and Immergut, E.H. (1989) *Polymer Handbook*, 3rd ed., New York; Wiley.
3. Chin, R.K., Beuth, J.L. and Amon, C.H. (1996) "Thermomechanical Modeling of Molten Metal Droplet Solidification Applied to Layered Manufacturing," *Mechanics of Materials*, Vol. 24, pp. 257-271.
4. Fessler, J.R., Merz, R., Nickel, A.H. and Prinz, F.B. (1996) "Laser Deposition of Metals for Shape Deposition Manufacturing," Proc. 1996 Solid Freeform Fabrication Symposium, Austin, August 1996, pp. 117-124.
5. Imasawa, Y. and Matsuo, M. (1970) "Fine Structures and Fracture Processes in Plastic-Rubber Two Phase Polymer Systems IV. Temperature and Strain Rate Dependencies of Tensile Properties," *Polymer Engineering and Science*, Vol. 10, No. 5, pp. 261-267.
6. Klingbeil, N.W. (1998) "Residual Stress-Induced Warping and Interlayer Debonding in Layered Manufacturing," Doctoral Thesis Dissertation, Carnegie Mellon University.
7. Klingbeil, N.W., Beuth, J.L., Chin, R.K, and Amon, C.H. (1998) "Measurement and Modeling of Residual Stress-Induced Warping in Direct Metal Deposition Process," *Solid Freeform Fabrication Proceedings* (D.L. Bourell, J.J. Beaman, H.L. Marcus, R.H. Crawford and J.W. Barlow, eds.), Proc. 1998 Solid Freeform Fabrication Symposium, Austin, August 1998, pp. 367-374.
8. Klingbeil, N.W., Beuth, J.L., Chin, R.K., and Amon, C.H. (2000) "Residual Stress-Induced Warping in Direct Metal Solid Freeform Fabrication," *International Journal of Mechanical Sciences*, submitted for publication.
9. Klingbeil, N.W., Zinn, J.W. and Beuth, J.L. (1997) "Measurement of Residual Stresses in Parts Created by Shape Deposition Manufacturing," *Solid Freeform Fabrication Proceedings* (D.L. Bourell, J.J. Beaman, H.L. Marcus, R.H. Crawford and J.W. Barlow, eds.), Proc. 1997 Solid Freeform Fabrication Symposium, Austin, August 1997, pp. 25-132.
10. Locati, G., Poggio, S., and Rathenow, J. (1996) "Evaluation of Thermal Behavior for Plastics," *Raw Materials & Applications*, Vol. 2, pp. 63-66.
11. Merz, R., Prinz, F.B., Ramaswami, K., Terk, M. and Weiss, L.E. (1994) "Shape Deposition Manufacturing," Proc. 1994 Solid Freeform Fabrication Symposium, Austin, August 1994, pp. 1-8.
12. Murray, G.T (1997) *Handbook of Materials Selections for Engineering Applications*, New York, M. Dekker, p. 214.